

Figure 1. CryoEM reconstruction of CA-SP1 assemblies: Fourier Shell Correlation (FSC) plot of 3D density map. The map resolution is 8.4 Å at FSC of 0.143.

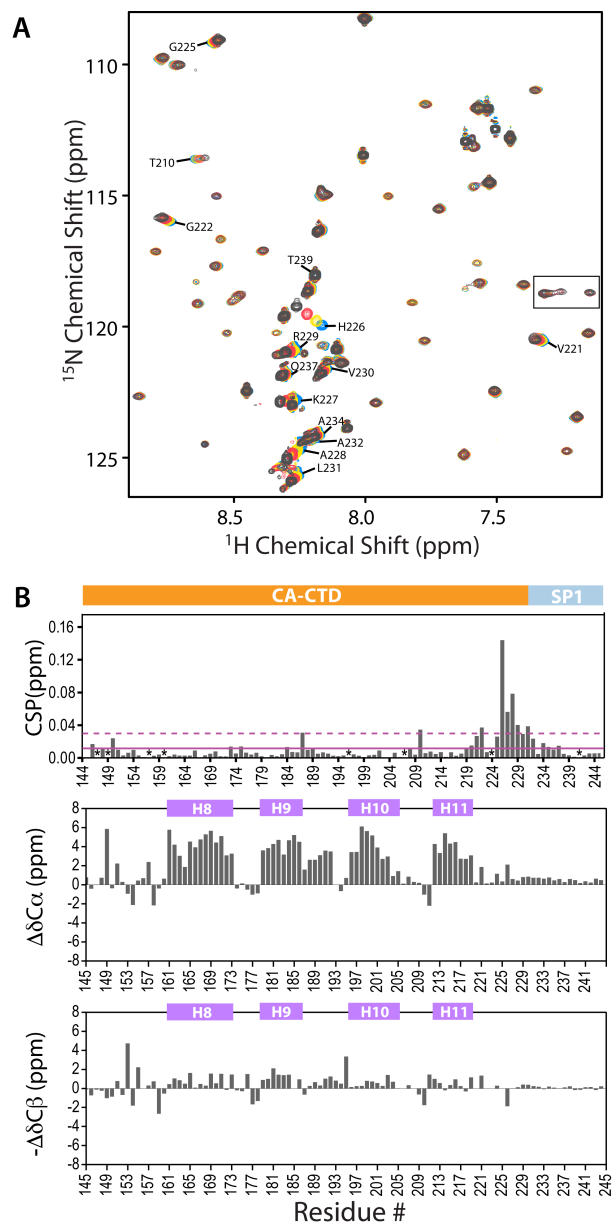


Figure 2. DFH-055 methanesulfonate binding to CA-CTD-SP1 (A) Superposition of a selective region of the ¹H-¹⁵N HSQC spectra of 1.11 mM CA-CTD-SP1 in the absence (blue) and presence (yellow), 2.22 mM (red) and 3.33 mM (black) DFH-055 methanesulfonate at 298K, 800 MHz. Representative CA-CTD-SP1 resonances are labeled with residue names and numbers. Folded arginine side chain N_ε resonances are enclosed in the rectangle. (B) Top: ¹H,¹⁵N-combined chemical shift changes, plotted along the linear amino acid sequence, were calculated using the equation $(\Delta\delta_{HN}^2 + (0.15\Delta\delta_N)^2)^{1/2}$, with $\Delta\delta_{HN}$ and $\Delta\delta_N$ representing ¹HN and ¹⁵N chemical shift differences between CA-CTD-SP1 resonances in the absence and presence (3.33 mM) of DFH-055 methanesulfonate, respectively. The solid and dashed horizontal lines indicate the average chemical shift change (0.011 p.p.m.) and the sum (0.030 p.p.m.) of the average change plus one S.D., respectively. Proline residues and the unassigned S149 positions are marked with *. Middle and bottom panels: Secondary chemical shifts (ΔC_{α} , middle; and $-\Delta C_{\beta}$, bottom) of CA-CTD-SP1 in solution. ΔC_{α} and ΔC_{β} were calculated by subtracting random coil C_α and C_β shifts¹ from the measured values.

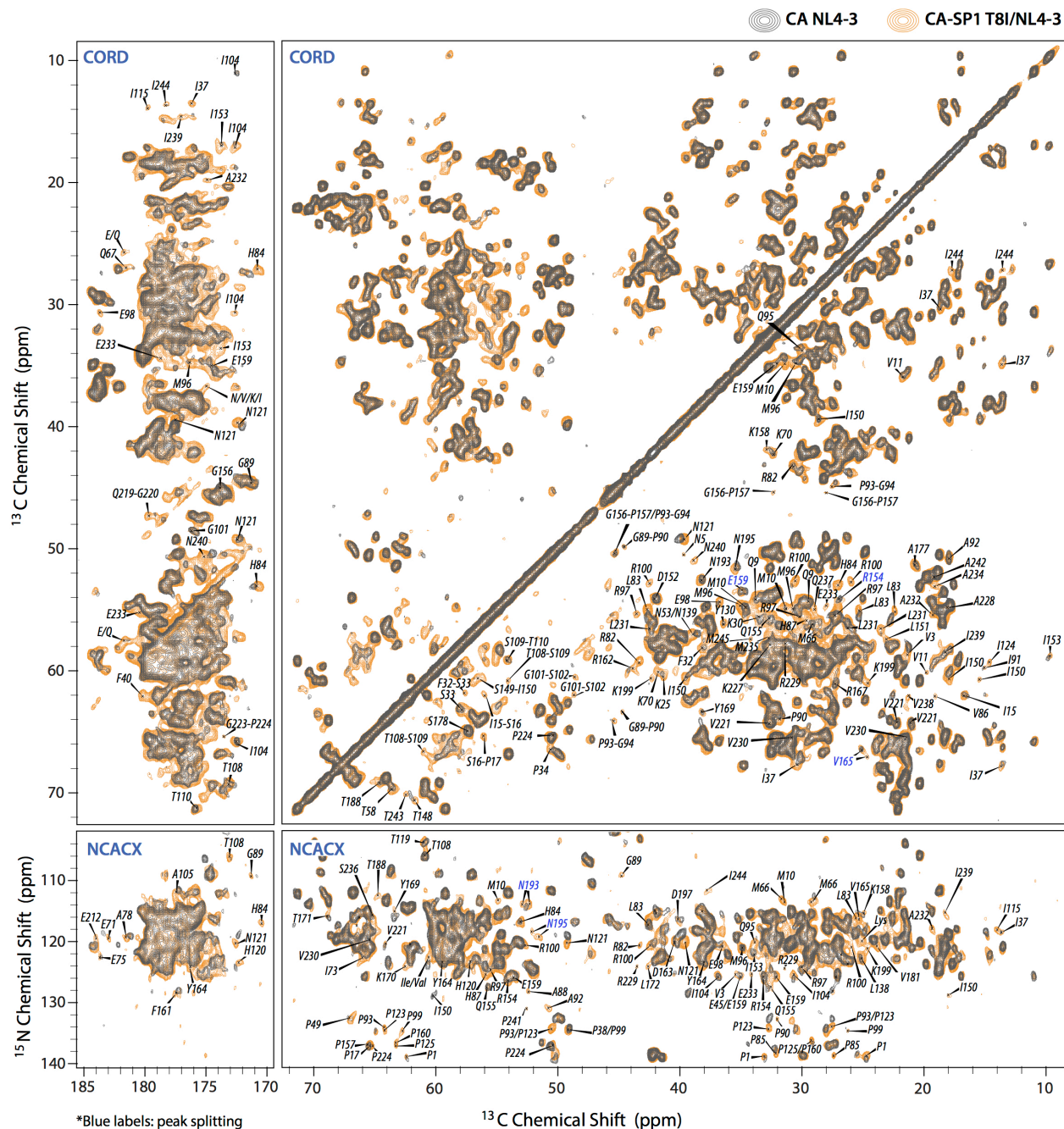
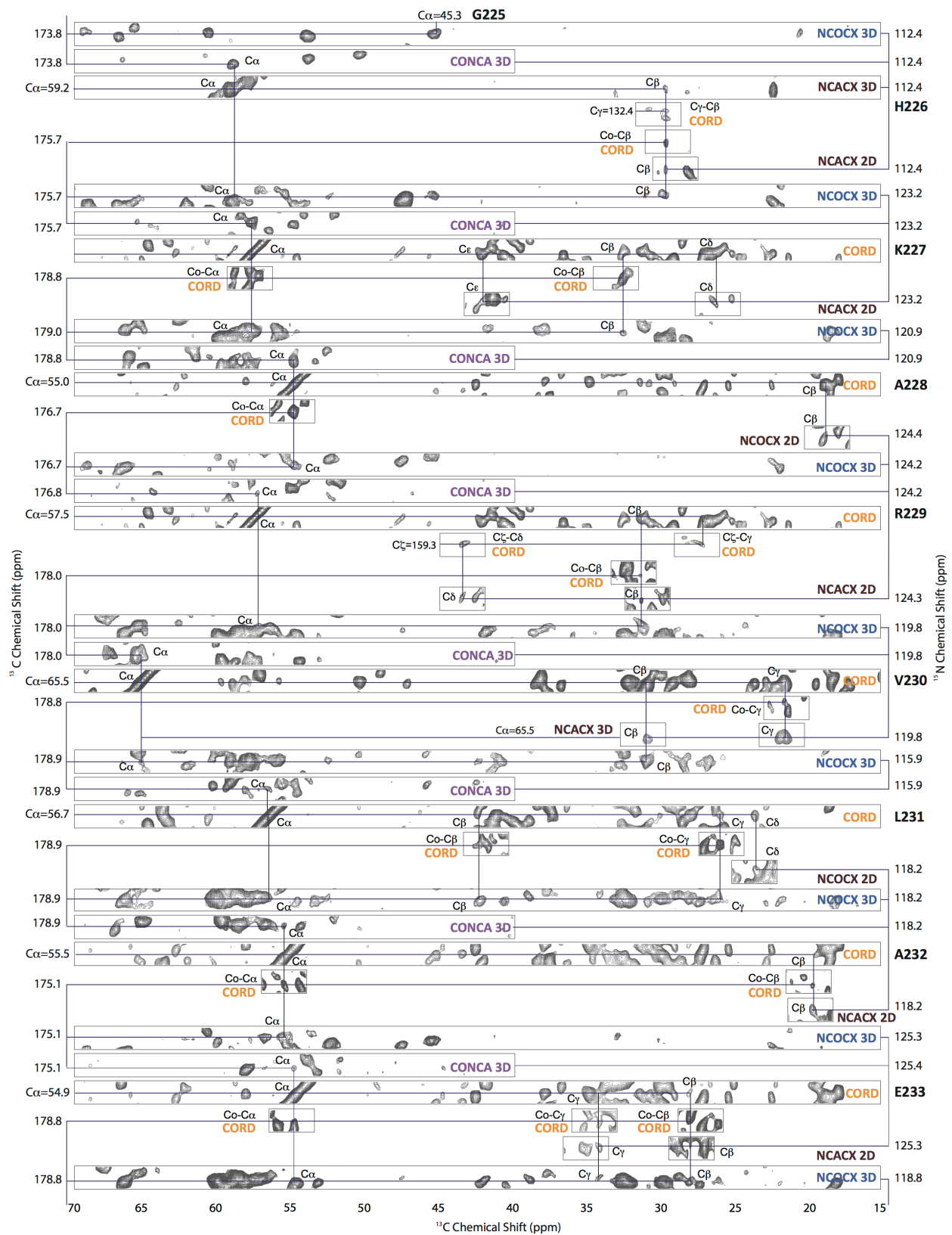
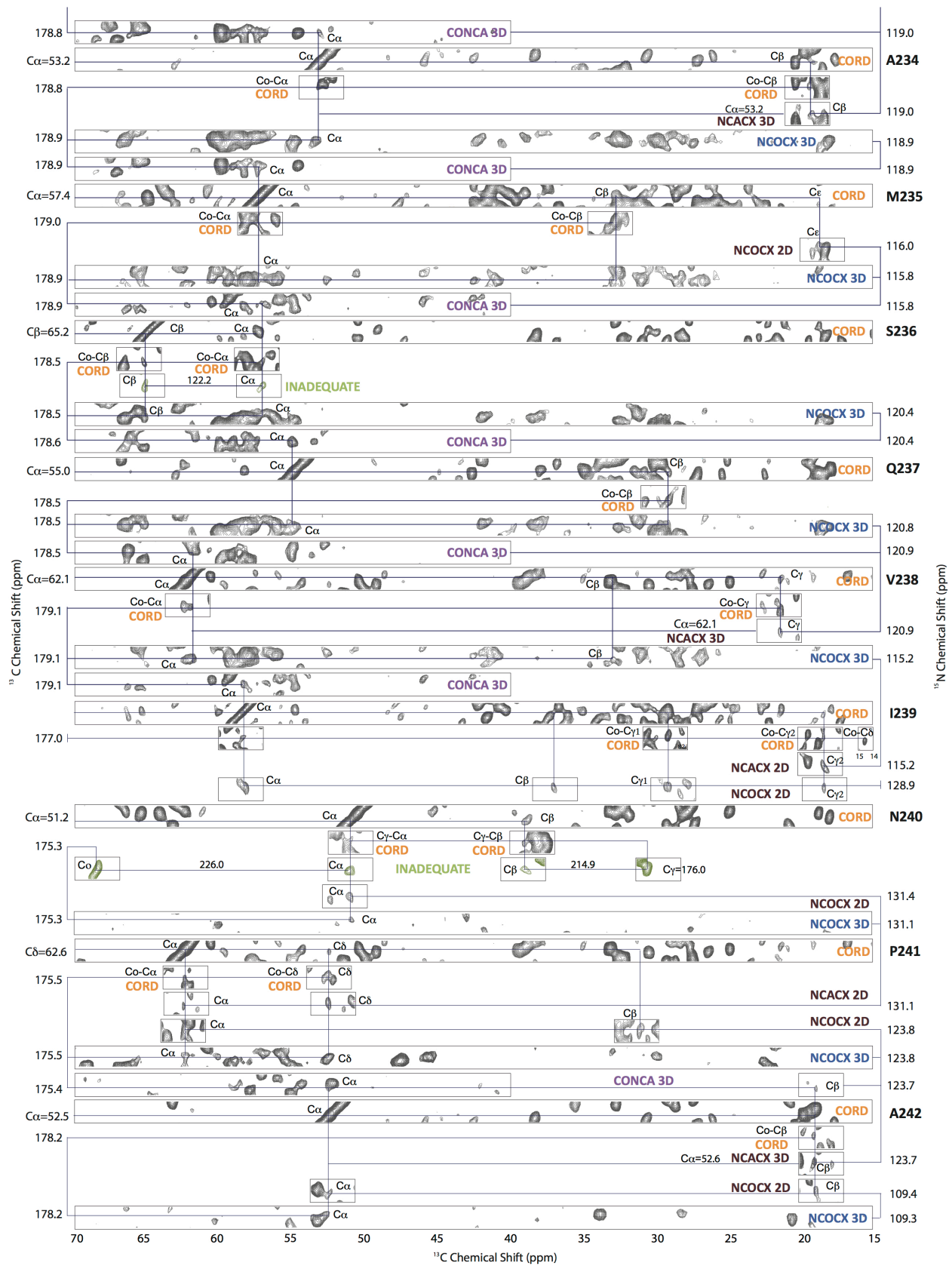


Figure 3. Comparison of dipolar-based spectra of HIV-1 CA and CA-SP1 T8I tubular assemblies. 2D CORD (top) and NCACX (bottom) MAS NMR spectra for CA NL4-3 (gray) and CA-SP1 NL4-3 T8I (orange), illustrating the multiple chemical shift and peak intensity changes. Residues for which resonance doubling is observed are labeled in blue. All spectra were acquired at 20.0 T with a MAS frequency of 14 kHz, and processed with 60° shifted sine bell apodization in both dimensions.





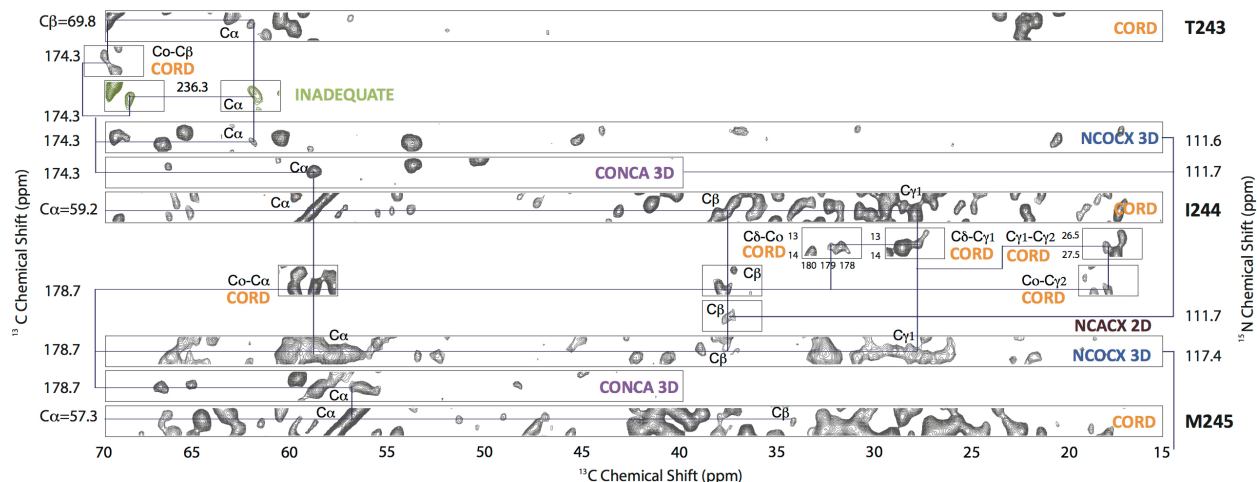


Figure 5. Sequential walk through the CTD-SP1 region for residues V221 to M245 in CA-SP1 NL4-3 T81 tubular assemblies. Resonances for this stretch of residues were assigned by a combination of several types of MAS NMR spectra: 2D CORD (orange labels), 2D/3D(NUS) NCACX (brown labels), 2D/3D NCOCX (brown / blue labels, respectively), 3D CONCA (purple labels), and 2D direct-INADEQUATE (green labels).

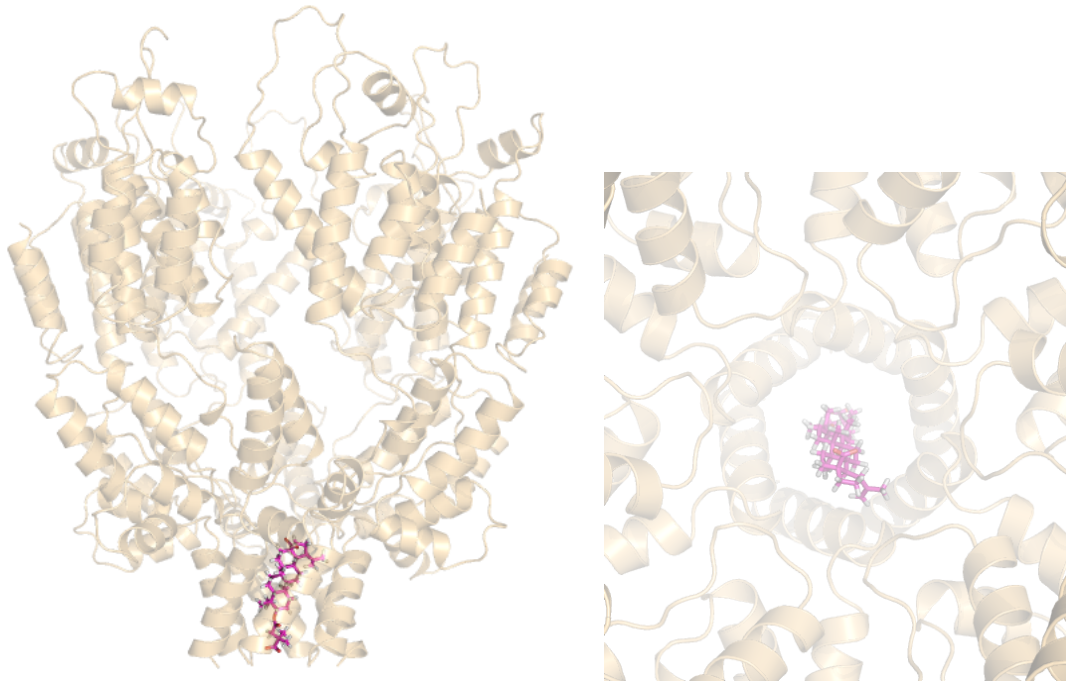


Figure 6. A binding pose of BVM (magenta) in the CTD-SP1 hexamer (X-ray structure PDB code 5L93) resulting from rigid body docking. Left: view from the side; right: view from the top.

Table 1. Experimental MAS NMR chemical shifts for the CTD-SP1 region (residues 221-245) of CA-SP1 T8I assemblies.

Residue	N	CO	CA	CB	CG	CD	CE	CZ	CSI 2.0
V221	120.53	176.98	64.29	32.72	22.18/21.04	-	-	-	C
G222	117.30	173.75	45.13	-	-	-	-	-	C
G223	112.59	173.82	45.23	-	-	-	-	-	C
P224	137.09	177.61	65.34	32.38	28.05	50.41	-	-	C
G225	116.27	173.80	45.35	-	-	-	-	-	C
H226	112.55	175.70	59.31	29.88	132.41	-	-	-	H
K227	123.19	179.00	57.90	32.59	26.16	29.89	42.09	-	H
A228	120.89	176.71	54.88	18.09	-	-	-	-	H
R229	124.17	177.96	57.54	31.37	27.10	43.63	-	159.28	H
V230	119.79	178.86	65.47	31.27	21.72	-	-	-	H
L231	115.90	178.92	56.83	42.34	26.23	23.47	-	-	H
A232	118.24	175.09	55.70	19.55	-	-	-	-	H
E233	125.35	178.80	54.89	28.09	34.11	-	-	-	H
A234	118.88	178.90	53.14	19.10	-	-	-	-	H
M235	118.89	179.03	57.42	32.54	-	-	18.64	-	H
S236	115.76	178.53	57.05	65.20	-	-	-	-	H
Q237	120.47	178.52	54.99	29.04	-	-	-	-	H
V238	120.50	179.06	62.10	33.09	21.22	-	-	-	C
I239	115.29	177.05	58.52	36.85	29.17/18.26	14.6	-	-	C
N240	128.80	175.30	51.10	39.13	176.00	-	-	-	C
P241	131.10	175.52	62.57	31.21	28.78	52.57	-	-	C
A242	123.70	178.19	52.54	18.92	-	-	-	-	C
T243	109.60	174.40	62.20	69.82	-	-	-	-	C
I244	111.60	178.65	59.22	37.75	27.59/17.87	13.77	-	-	C
M245	117.40	-	57.33	34.16/33.69	-	-	-	-	C

Table 2. Secondary structure predictions for the CTD-SP1 region (residues 221-245) determined by MAS NMR for different CA-SP1 variants. CSI 2.0² and TALOS-N³ programs were used to predict secondary structures from the chemical shift index (CSI) and torsion angles, respectively. Designations C-coil and H-helix are as described in Materials and Methods.

Residue	NL4-3/T8I		NL4-3/A92E		HXB2		NL4-3/solution NMR	
	CSI 2.0	TALOS-N	CSI 2.0	TALOS-N	CSI 2.0	TALOS-N	CSI 2.0	TALOS-N
V221	C	C	C	C	C	C	C	C
G222	C	C	C	C	C	C	C	C
G223	C	C	C	C	C	C	C	C
P224	C	C	-	-	-	C	C	C
G225	C	C	-	-	-	C	C	C
H226	H	H	C	-	C	C	C	C
K227	H	H	C	C	C	-	C	C
A228	H	H	C	-	-	-	C	C
R229	H	H	C	H	C	-	C	C
V230	H	H	H	H	-	-	C	C
L231	H	H	H	H	C	-	C	C
A232	H	H	H	H	H	-	C	C
E233	H	H	H	H	H	H	C	H
A234	H	H	C	-	H	-	C	H
M235	H	H	C	-	-	-	C	C
S236	H	H	C	-	-	-	C	C
Q237	H	C	C	-	-	-	C	C
V238	C	C	-	-	-	-	C	C
I239/T239	C	C	C	-	C	-	C	C
N240	C	C	C	-	-	-	C	C
P241	C	C	-	-	-	-	H	C
A242	C	C	C	-	C	-	H	C
T243	C	C	C	-	-	-	H	C
I244	C	C	C	-	-	-	C	C
M245	C	C	C	-	-	-	C	C

“-“ The predictions are less reliable due to the missing chemical shifts.

Table 3. Secondary structure predictions for the NTD in CA-SP1 assemblies by MAS. CSI 2.0² and TALOS-N³ programs were used to predict secondary structures from the chemical shift index (CSI) and torsion angles, respectively.

Residue	NL4-3/T8I		NL4-3/A92E		HXB2	
	CSI 2.0	TALOS-N	CSI 2.0	TALOS-N	CSI 2.0	TALOS-N
P1	C	C	C	-	C	C
I2	B	C	B	-	B	C
V3	B	B	B	B	B	B
Q4	B	B	C	B	C	B
N5	C	C	C	C	C	C
L6/I6	H	H	C	C	C	H
Q7	C	H	C	H	C	H
G8	C	H	H	H	C	H
Q9	C	C	C	C	C	C
M10	C	B	B	B	B	B
V11	B	B	B	B	B	B
H12	B	B	B	B	B	B
Q13	B	B	B	B	B	B
A14	C	B	B	B	B	B
I15	C	C	C	C	C	C
S16	C	C	C	C	C	C
P17	H	H	H	H	H	H
R18	H	H	H	H	H	H
T19	H	H	H	H	H	H
L20	H	H	H	H	H	H

“-“ The predictions are less reliable due to the missing chemical shifts.

Table 4. Temperature rungs and its associated weights used for the simulated-tempering simulation of wild-type CA-SP1.

Temperature Rung (K)	Simulated Tempering Weight
310.0	-30301.841
313.5	-26789.562
317.0	-23365.365
320.5	-20026.189
324.0	-16769.137
327.5	-13591.374
331.0	-10490.412
334.5	-7463.558
338.0	-4508.334
341.5	-1622.494
345.0	1196.552
348.5	3951.036
352.0	6642.746
355.5	9273.551
359.0	11845.700
362.5	14360.941
366.0	16820.933
369.5	19227.457
373.0	21582.033
376.5	23886.104
380.0	26141.213

Table 5. Temperature rungs and associated weights used in the simulated-tempering simulation (REF) of the CA-SP1(T8I) mutant.

Temperature Rung (K)	Simulated Tempering Weight
310.0	-30503.934
313.5	-26969.450
317.0	-23523.689
320.5	-20163.410
324.0	-16885.355
327.5	-13686.826
331.0	-10565.196
334.5	-7517.995
338.0	-4542.650
341.5	-1636.687
345.0	1201.979
348.5	3975.335
352.0	6685.528
355.5	9335.030
359.0	11925.878
362.5	14459.436
366.0	16937.267
369.5	19361.216
373.0	21732.931
376.5	24054.204
380.0	26326.389

REFERENCES

- 1 Wishart, D. S., Bigam, C. G., Holm, A., Hodges, R. S. & Sykes, B. D. ^1H , ^{13}C and ^{15}N random coil NMR chemical shifts of the common amino acids. I. Investigations of nearest-neighbor effects. *J Biomol NMR* **5**, 67-81, doi:10.1007/bf00227471 (1995).
- 2 Hafsa, N. E. & Wishart, D. S. CSI 2.0: a significantly improved version of the Chemical Shift Index. *J Biomol NMR* **60**, 131-146, doi:10.1007/s10858-014-9863-x (2014).
- 3 Shen, Y. & Bax, A. Protein Backbone and Sidechain Torsion Angles Predicted from NMR Chemical Shifts using Artificial Neural Networks. *J Biomol NMR* **56**, 227-241, doi:10.1007/s10858-013-9741-y (2013).